

## NUMERICAL MODELLING OF THE QUASI-GLOBAL OCEAN CIRCULATION BASED ON POM\*

XIA Chang-shui

Key Laboratory of Marine Science and Numerical Modeling, The First Institute of Oceanography, State Oceanic Administration, Qingdao 266061, China

The Marine Environment College, Ocean University of China, Qingdao 266003, China,  
 e-mail: xiachsh@fio.org.cn

QIAO Fang-li, ZHANG Qing-hua, YUAN Ye-li

Key Laboratory of Marine Science and Numerical Modeling, The First Institute of Oceanography, State Oceanic Administration, Qingdao 266061, China

(Received Feb. 8, 2004)

**ABSTRACT:** A free surface quasi-global ocean circulation model, Princeton Ocean Model (POM), was adopted to simulate the climatological circulation. The horizontal resolution of the model was  $1/2^\circ \times 1/2^\circ$  with 16 vertical sigma layers. The initial temperature and salinity fields of the model were interpolated from the Levitus data, and the COADS (Comprehensive Ocean-Atmosphere Data Set) monthly mean SST and wind fields were used as the surface forcing. The integral time length is 6a. The main general circulation components such as the equatorial current, the equatorial undercurrent, the south and north equatorial currents, the Antarctic Circumpolar Current (ACC), the Kuroshio and the Gulf Stream were well reconstructed. The volume transports of PN section and ACC agree well with the estimations on field survey. Up to now there is no global or quasi-global circulation model results using POM in literature. Our results demonstrate that POM has sound ability to simulate the coastal circulation as well as the general ocean circulation. And this result can provide open boundary conditions for fine resolution regional ocean circulation models.

**KEY WORDS:** ocean circulation, numerical model, Princeton Ocean Model (POM)

### 1. INTRODUCTION

Ocean circulation is the core of physical oceanography. To improve the understanding of ocean circulation has significant influence on human activities such as navigation, military, and fishing. There are mainly three methods in the study of ocean circulation: the first is field survey, the second is the theoretical study using the simplified

governing equations and the third is numerical modeling. The rapid development of computer technology made it possible to simulate the global ocean circulation using the three-dimensional primitive equation ocean numerical model with fine horizontal resolutions. Li et al.<sup>[1]</sup> discussed the ocean responses to different external forcing on L30T63. Fujio et al.<sup>[2-3]</sup> calculated the global diagnostic circulation with the horizontal resolution of  $2^\circ \times 2^\circ$  so the marginal seas were not well distinguished. Wei et al.<sup>[4]</sup> ran a global diagnostic ocean circulation model (MOM2) with  $1^\circ \times 1^\circ$  horizontal resolution, the main circulation patterns were well simulated in the result and the water mass, and heat and salinity fluxes through representative sections were analyzed but with rigid surface approximation. Although the free surface POM costs much more CPU time than that of rigid surface approximation, the POM has still been widely used in the coastal circulation modeling, and one of the important reasons is that the Mellor-Yamada<sup>[5]</sup> turbulence closure model can supply the vertical kinematic viscosity/diffusivity. Qiao et al.<sup>[6]</sup> studied the path and the origin of the Yellow Sea Warm Current (YSWC) with the POM. However, The POM was successfully applied to large-scale ocean circulation modeling recently. Kagimoto and Yamagata<sup>[7]</sup> applied the POM to the circulation modeling of the whole Pacific. Ezer and Mellor<sup>[8]</sup> simulated the climatology circulation of the whole At-

\* Project supported by the Major State Basic Research Program of China (Grant No: G1999043809).

lantic. Guo<sup>[9]</sup> studied the effects of different horizontal resolutions and JEBAR on Kuroshio using a triply nested model based on POM, and the maximum model domain included almost all the Pacific. As known to the authors, up to now there is no global or quasi-global circulation model results of the POM in literature. Herein a quasi-global circulation model based on the POM with horizontal resolution of  $1/2^\circ \times 1/2^\circ$  is set up to simulate the global climatology circulation. It can provide open boundary conditions for fine resolution regional ocean circulation models<sup>[10-14]</sup>.

## 2. MODEL DESCRIPTION

The model domain is between  $78^\circ\text{S}$ - $65^\circ\text{N}$ . 16 sigma levels are used in the vertical direction (Table 1), and high vertical resolution is for the upper ocean. Cyclic boundary condition is used in the west-east boundary and the solid boundary conditions are used for the north and south boundaries for simplicity. The topography of the model is interpolated from the global  $5^\circ \times 5^\circ$  Etopo5 with the following two modifications:

(1) Setting the minimum of 10m and maximum of 3000 m in the model.

(2) Smoothing the topography satisfying the following criteria (Mellor et al.<sup>[15]</sup>):

$$\frac{|H_{i+1} - H_i|}{(H_{i+1} + H_i)} \quad (1)$$

where  $H_{i+1}$  and  $H_i$  are the depths at two adjacent grids and  $\alpha$  is a slope factor and set as 0.2 here.

**Table 1 Vertical layers of the circulation model**

layer	value	layer	value
1	0.00000	9	- 0.30000
2	- 0.00313	10	- 0.40000
3	- 0.00625	11	- 0.50000
4	- 0.01250	12	- 0.60000
5	- 0.02500	13	- 0.70000
6	- 0.05000	14	- 0.80000
7	- 0.10000	15	- 0.90000
8	- 0.20000	16	- 1.00000

The initial temperature and salinity are set to be the Levitus annually mean values, to reduce the error of the horizontal baroclinic pressure gradient, the horizontal mean density is subtracted before the calculation of the horizontal baroclinic pressure gradient and the horizontal mean density is set to be the annually mean density field. The  $1^\circ \times 1^\circ$  COADS monthly mean SST field and wind stress (Arlindo de Silva) are used as surface forcing. Similar to Fang and Wei's work<sup>[16]</sup>, the model is integrated for 6a and the monthly mean results of the last year are used to study the quasi-global climatology circulation.

## 3. MODEL RESULTS

### 3.1 The stream function

The definition of stream function is

$$u = - \frac{\partial \psi}{\partial y}, \quad v = \frac{\partial \psi}{\partial x}$$

where  $u$ ,  $v$  is the eastern and northern current velocity components, respectively. The value of the stream function along the north boundary is set to be zero. The calculated annually mean stream function is shown in Fig. 1. This distribution is similar to the results of Fujio et al.<sup>[2,3]</sup> and Wei et al.<sup>[4]</sup>. The characteristics of the stream function in the northern hemisphere are: the stream function is positive in the middle and low latitude areas and the maximum value is located at the center which suggests a clockwise circulation. The stream function is negative in the high latitude areas with minimum value at the center which suggests an anti-clockwise circulation. In the southern hemisphere the circulation between  $40^\circ\text{S}$  -  $60^\circ\text{S}$  is the ACC, the stream function contours are almost parallel and intense. Between the ACC and the equator the stream function is negative and the minimum value is located at the center which suggests an anti-clockwise circulation.

The stream function near the west boundaries of each ocean is intense, so the west intensification character is clear. Compared with the results of Fujio et al.<sup>[2,3]</sup> and Wei et al.<sup>[4]</sup>, the simulated width of the west boundary currents such as the Kuroshio and the gulf stream is narrow and the corresponding maximum velocity are larger, those characters are insistent with observations. The

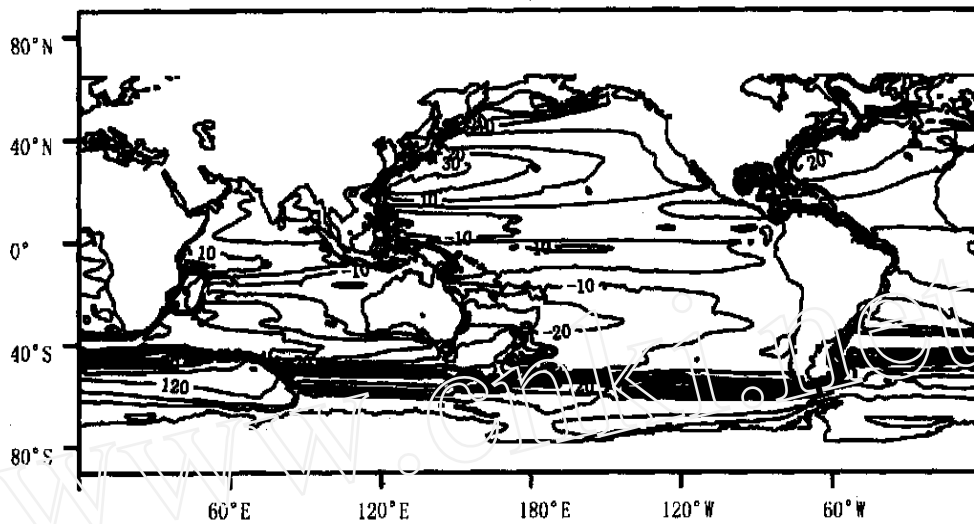


Fig. 1 The simulated annual mean stream function (unit :Sv)

simulated annual mean transport through the P-N section of the Kuroshio in the East China Sea is 25Sv while the observation deduced from temperature and salinity is 25.4Sv by Hinata<sup>[17]</sup>, however, the simulated Kuroshio current speed is weak and the width is larger than the observation because the  $1/2^\circ \times 1/2^\circ$  horizontal resolution is still too coarse. The simulated transport of the gulf stream is 40Sv-50Sv which is close to the results of Fujio et al.<sup>[2-3]</sup> and Wei et al<sup>[4]</sup>.

### 3.2 Mean sea level distribution

The simulated annual mean sea level is shown in Fig. 2 (a) (the contour interval is 0.1m). The simulated annual mean sea level of the OCCAM (the Southampton Oceanography Centre, UK) is shown in Fig. 2 (b) with the horizontal resolution of  $1/4^\circ \times 1/4^\circ$  (drawn using the data from the OCCAM web site <http://www.soc.soton.ac.uk/JRD/OCCAM/welcome.html>). The patterns of the two results are much similar. The main characteristics are that in the southern hemisphere, the sea level of ACC between  $40^\circ\text{S}$ - $70^\circ\text{S}$  is negative and becomes lower to the high latitude. In the northern hemisphere in the area between  $40^\circ\text{N}$ - $60^\circ\text{N}$  the value of sea level is also negative with the minimum value at the center which corresponds to the anti-clockwise circulation in this area. Except the areas mentioned above, the sea level is positive. In the Pacific the sea level distribution pattern is somewhat like a "W" which rotates  $90^\circ$  clockwise,

and there are two-maximum areas besides the equator which coincides with the clockwise circulation in the middle and low latitude area in the northern hemisphere and the anti-clockwise circulation in the middle and low latitude area in the southern hemisphere. The sea level distribution in the Atlantic is similar to that of the Pacific. The sea level contours are very intense in west boundaries of the Pacific and Atlantic oceans, which suggests the west intensification of the ocean circulation. The horizontal resolution of the OCCAM is  $1/4^\circ \times 1/4^\circ$ , so in strong current areas such as the Kuroshio the sea level gradient is larger than our results.

### 3.3 The upper ocean circulation

#### 3.3.1 The Pacific Ocean

Circulation in the North Pacific Ocean:

The simulated annual mean horizontal current at depth of 20m is shown in Fig 3. In the high latitude area ( $40^\circ\text{N}$ - $60^\circ\text{N}$ ) there is an anti-clockwise circulation gyre which includes the Oyashio, the North Pacific Current and the Alaska current. In the middle and low latitude area ( $10^\circ\text{N}$ - $40^\circ\text{N}$ ) there exists a clockwise circulation composed of the North Equatorial Current, the Kuroshio, the Kuroshio Extension, the North Pacific Current and the California Current. The North Equatorial Current flows from the east to west between  $10^\circ\text{N}$ - $20^\circ\text{N}$  and it splits into two branches when it reaches the west bank of the Pacific. One part of the south branch

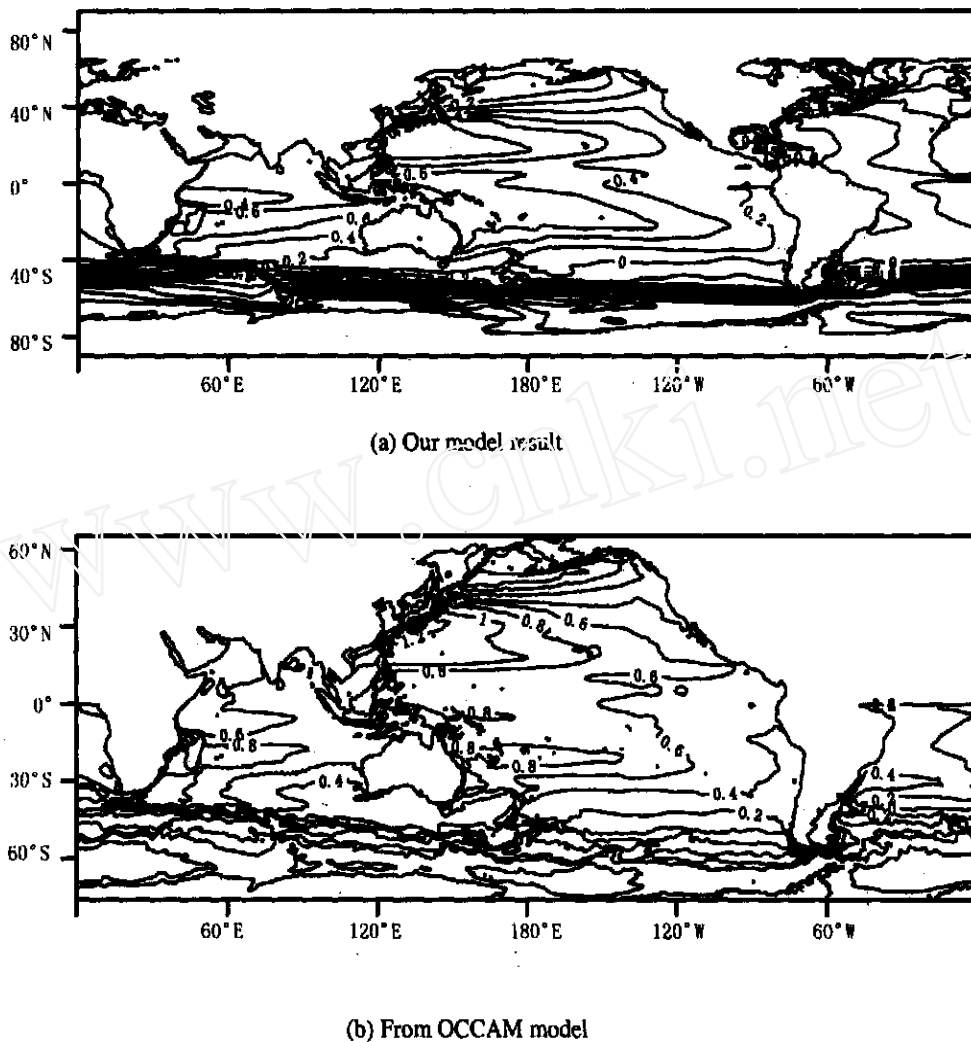


Fig. 2 The simulated annual mean sea levels (unit :m)

flows into the North Equatorial Counter Current, the other part of the south branch enters the Indonesian Sea, flows into the Indian Ocean and constitutes the main part of the Pacific-Indian Through Flow. The Pacific-Indian Through Flow will not be discussed here since the horizontal resolution of the model is not high enough. The north branch of the North Equatorial Current turns north along the west coast and forms the Kuroshio. A small portion of the Kuroshio enters the South China Sea when it passes by the east of Luzon Straits, the rest larger part intrudes the East China Sea from the east of the Taiwan Island and flows northeast approximately along the topography contour of 200m. The Kuroshio turns into two parts in the north of the Ryukyu Islands: a small part enters the Sea of Japan through the Tsushima Strait, the rest larger portion turns clockwise and flows

out of the East China Sea through the Tokara Strait. The Kuroshio turns northeast along the south Japan Coast and flow into the North Pacific Current eastward near  $38^{\circ}$  blocked by the southward Oyashio. The speed of the current reduces gradually as it flows to the east of the Pacific. It turns southward near California blocked by the east bank and enters the North Equatorial Current again, so it forms a large clockwise circulation circle.

#### The Equator Circulation System :

Figure 4 (a) shows the simulated zonal current of the  $155^{\circ}\text{W}$  section, and combined with Fig. 3 it is shown that in the upper layer of 0-100m and between  $5^{\circ}\text{S}$  and  $5^{\circ}\text{N}$  the strong Equatorial Current flows from the east to west with the maximum speed up to 0.7m/s-0.8m/s. Between  $5^{\circ}\text{N}$  and  $10^{\circ}\text{N}$  is the North Equatorial Countercurrent while the

North Equatorial Current is located between 10°N and 20°N. The North Equatorial Countercurrent and the North Equatorial Current form an anti-clockwise circle. The zonal current along the 155°W section derived from measured temperature and salinity data (Wyrtki and Kobalinsky<sup>[18]</sup>) is shown in Fig. 4(b), compared with the simulated results in Fig. 4(a). The distribution pattern of the Equatorial Current, the Equatorial Countercurrent and the Equatorial Undercurrent is similar to each other, but the simulated width of the Equatorial Undercurrent is still larger and the speed is lower than the observations, which may be due to the low model horizontal resolution. Compared with the updated simulation (Fig. 3 of Fang et al.<sup>[19]</sup>), the simulated Equatorial Undercurrent is mainly located 80m-40m and the north Equatorial Countercurrent 0-180m. Our simulation fits well with observations (Fig. 4(b)).

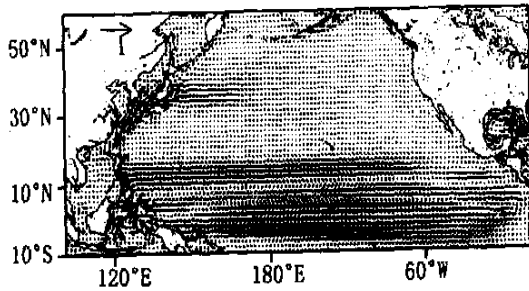


Fig. 3 The simulated annual mean velocity field at the depth of 20m between 10°S-60°N of the Pacific Ocean (unit: m/s)

Circulation in the South Pacific :

The simulated annual mean horizontal current at the depth of 20m in the South Pacific is shown in Fig. 5. In the South Pacific, there exists an anti-clockwise circulation circle including the South Equatorial Current in low latitude, the East Australian Current along the eastern Australian coast, the ACC in the South and the Peru current along the east coast of the South Pacific.

3.3.2 The Indian Ocean

The simulated upper ocean circulation patterns in summer and winter of the Indian Ocean are shown in Figs. 6 and 7 respectively. The bathymetry of the Indian Ocean is different from those of the Pacific and the Atlantic, its horizontal scale is much smaller, and the upper ocean circulation is controlled by the Indian monsoon. In summer there is a clockwise circulation in the north

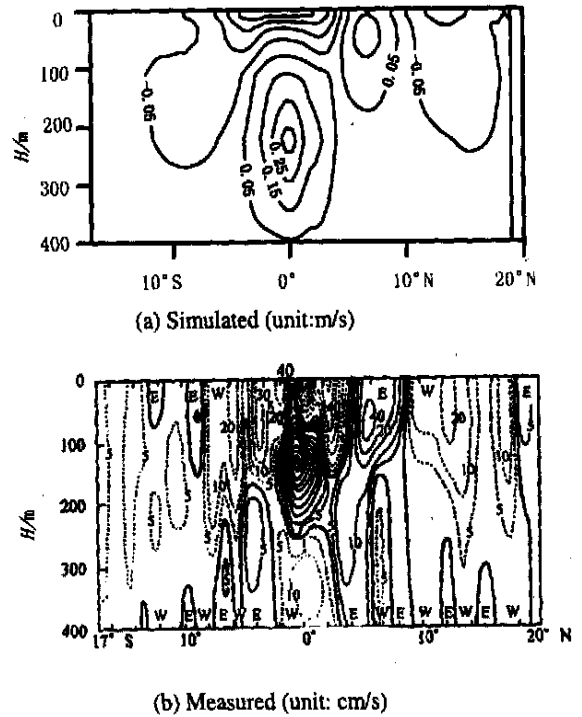


Fig. 4 Simulated zonal velocity field (unit: m/s)

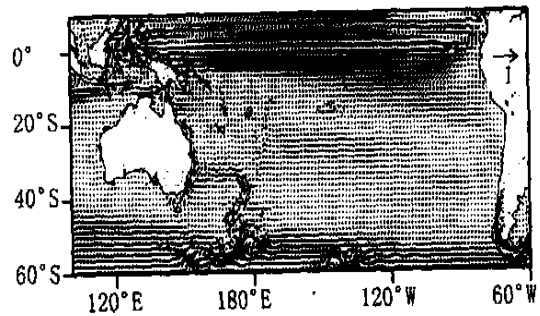


Fig. 5 The simulated annual mean velocity field at the depth of 20m between 60°S-10°N of the Pacific Ocean (unit: m/s)

Indian Ocean (10°N-20°N) but in winter there is an anti-clockwise circulation due to the Indian monsoon, and the clockwise circulation circle only exists in the Bangladeshi Bay. An anti-clockwise circulation exists in the southern Indian Ocean all year around.

3.3.3 The Atlantic Ocean

The simulated annual mean currents at the depth of 20m in the North Atlantic Ocean and the South Atlantic Ocean are shown in Figs. 8 and 9, respectively. The simulated results agree with common understanding of the circulation pattern of the Atlantic. In the southern subtropics area, there is an anti-clockwise circulation including the South

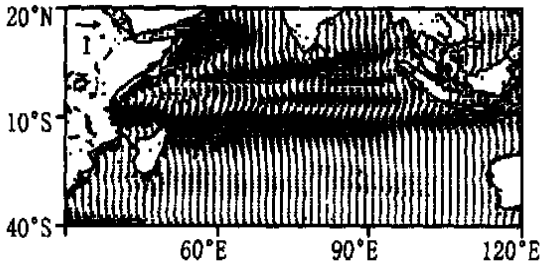


Fig. 6 The simulated boreal winter (Feb.) velocity field at the depth of 20m in the India Ocean (unit :m/ s)

Equatorial Current in the north , the Brazilian Current in the west , the ACC in the south and the Benguela Current in the east. In the northern subtropics area , there is a clockwise circulation including the North Equatorial Current , the Gulf Stream , the North Atlantic Current and the Canaries Current along the east coast of North Atlantic. Similar to the Pacific , there also exists the South and North Equatorial Currents and the Equatorial Countercurrent in the tropical area.

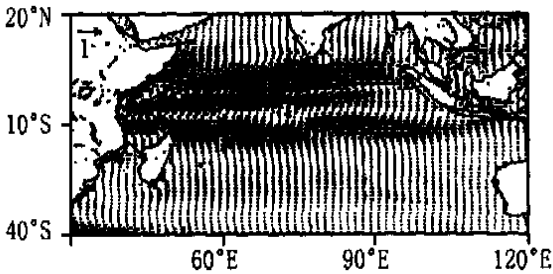


Fig. 7 The simulated boreal summer (Aug.) velocity field at the depth of 20m in the Indian Ocean (unit :m/ s)

### 3.3.4 The ACC

The ACC is the only meridian boundless current in the globale ocean with 15000km long , strong and deep , and the width of ACC extents to 2500km. Driven by the powerful west wind it flows from west to east from the sea surface to the deep ocean with the depth about several thousand meters. The ACC occupies the most of southern ocean , and is the most powerful ocean current in the globe. The simulated annual mean transport of the ACC through the Drake Straits is 195Sv , which agrees well with the result of the FRAM (website <http://www.mth.usa.ac.uk/ocean/fram.html>).

## 4. CONCLUSIONS

The climatological ocean circulation has been simulated based on the free surface POM with the horizontal resolution of  $1/2^\circ \times 1/2^\circ$ . All the main

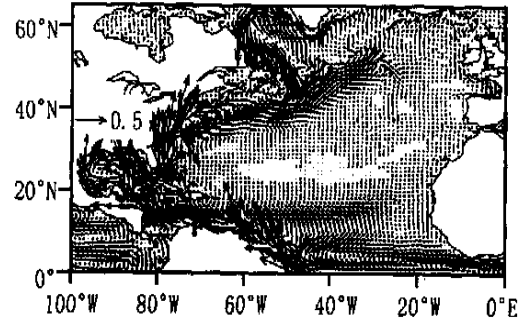


Fig. 8 The simulated annual mean velocity field at the depth of 20m in the North Atlantic Ocean

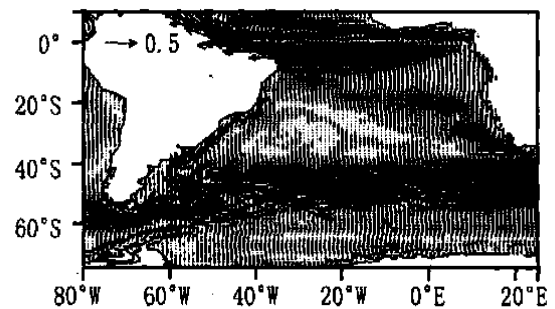


Fig. 9 The simulated annual mean velocity field at the depth of 20m in the South Atlantic Ocean

circulation systems have been well reproduced. Although the speed of some simulated strong currents such as the Kuroshio and the Gulf Stream is smaller and the width is larger than the observations , the main transports of Kuroshio , ACC , the Gulf Stream are still reasonable. This suggests the POM has sound ability to reconstruct the global circulation. The simulation of the tropical current system has been much improved. The result of this paper can provide reasonable boundary conditions for fine-resolution regional circulation models<sup>[10-14]</sup>.

## REFERENCES

- [1] LI Wei , LIU Ha-long , ZHANG Xue-hong et al. The response of the third generation of IAP/LASG oceanic GCM to different external forcing [J]. *Journal of Hydrodynamics, Ser. B*, 2001 , 13(3) : 107-114.
- [2] FUJIO S. et al. World ocean circulation diagnostically derived from hydrographic and wind stress fields 1 , The velocity field [J]. *J. Geophys. Res.* , 1992 , 97: 11163-11176.
- [3] FUJIO S. et al. World ocean circulation diagnostically derived from hydrographic and wind stress fields 2 , The water movement [J]. *J. Geophys. Res.* , 1992 , 97: 14439-14452.

- [4] WEI Ze-Xun, CHOI B. H. and FANG Guo-hong. Water, heat and salt transports from diagnostic world ocean and north Pacific circulation models[J]. *La Mer.*, 2000, 38(4): 211-218.
- [5] MELLOR G. L. and YAMADA T. Development of a turbulence closure model for geophysical fluid problems[J]. *Rev. Geophys. and Space Phys.*, 1982, 20: 851-875.
- [6] QIAO Fang-li, XU Xiao-biao, TANG Ya-xiang et al. A numerical study on the path and origin of the Yellow Sea Warm Current YSWC[J]. *Journal of Hydrodynamics, Ser. B*, 2001, 13(3): 1-9.
- [7] KAGIMOTO T. and YAMAGATA T. Seasonal transport variations of the Kuroshio: An OGCM simulation[J]. *J. Phys. Ocean.*, 1997, 27: 403-418.
- [8] EZER T. and MELLOR G. L. Simulation of the Atlantic Ocean with a free surface sigma coordinate ocean model [J]. *J. Geophys. Res.*, 1997, 102: 15647-15657.
- [9] GUO X. et al. A triply nested ocean model for simulating the Kuroshio-Roles of horizontal resolution and JEBAR [J]. *J. Phys. Oceanogr.*, 2003, 33: 146-169.
- [10] QIAO Fang-li, XIA Chang-shui, SHI Jiu-xin et al. Seasonal variability of thermocline in the Yellow Sea[J]. *Chinese J. Oceanology and Limnology*, 2004, 22(3): 299-305.
- [11] MA Jian and QIAO Fang-li. Simulation and analysis on seasonal variability of average salinity in the Yellow Sea [J]. *Chinese J. Oceanology and Limnology*, 2004, 22(3): 306-313.
- [12] MA Jian, QIAO Fang-li, XIA Chang-shui et al. Tidal effects on temperature front in the Yellow Sea[J]. *Chinese J. Oceanology and Limnology*, 2004, 22(3): 314-321.
- [13] YANG Yong-zeng, QIAO Fang-li, XIA Chang-shui et al. Wave-induced mixing in the Yellow Sea[J]. *Chinese J. Oceanology and Limnology*, 2004, 22(3): 322-326.
- [14] XIA Chang-shui, QIAO Fang-li, ZHANG Meng-ning et al. Simulation of double cold cores of the 35°N section in the Yellow Sea with a wave-tide-circulation coupled model [J]. *Chinese J. Oceanology and Limnology*, 2004, 22(3): 292-298.
- [15] MELLOR G. L. MECHOSO C. and KETO E. A diagnostic calculation of the general circulation of the Atlantic Ocean[J]. *Deep Sea Res.*, 1982, 29: 1171-1192.
- [16] FANG Guo-hong. and WEI Ze-xun. The volume, heat and salinity transport of the China Seas: the global model result[J]. *Science in China, Ser. D*, 2002, 32(12): 969-977. (in Chinese)
- [17] HINADA T. Seasonal variation and long-term trends of the oceanographic conditions along a fixed hydrographic line crossing the Kuroshio in the East China Sea[J]. *Oceanogr. Mag.*, 1996, 45: 9-32.
- [18] WYRTKI K. and KOBLENSKY B. Mean water and current structure during the Hawaii to Tahiti shuttle experiment[J]. *J. Phys. Ocean.*, 1984, 14: 242-254.
- [19] FANG Guo-hong. WEI Ze-xun, WANG Yong-gang. et al. An extended variable-grid global ocean circulation model and its preliminary results of the equatorial Pacific circulation[J]. *Acta Oceanologica Sinica*, 2004, 23(1): 23-30.

**Biography:** XIA Chang-shui (1974-), Male, Master, Assistant Researcher